Chapter 7

Review of Low Cycle Fatigue: Issues in Naval and Offshore Engineering

Chapter details

Chapter DOI:

https://doi.org/10.4322/978-65-86503-83-8.c07

Chapter suggested citation / reference style:

Morales, Leonel L. D., et al. (2022). "Review of Low Cycle Fatigue: Issues in Naval and Offshore Engineering". *In* Jorge, Ariosto B., et al. (Eds.) *Fundamental Concepts and Models for the Direct Problem*, Vol. II, UnB, Brasilia, DF, Brazil, pp. 184–208. Book series in Discrete Models, Inverse Methods, & Uncertainty Modeling in Structural Integrity.

P.S.: DOI may be included at the end of citation, for completeness.

Book details

Book: Fundamental Concepts and Models for the Direct Problem

Edited by: Jorge, Ariosto B., Anflor, Carla T. M., Gomes, Guilherme F., & Carneiro, Sergio H. S.

Volume II of Book Series in:

Discrete Models, Inverse Methods, & Uncertainty Modeling in Structural Integrity

Published by: UnB City: Brasilia, DF, Brazil Year: 2022

DOI: https://doi.org/10.4322/978-65-86503-83-8

Review of Low Cycle Fatigue: Issues in Naval and Offshore Engineering

Leonel Leonardo Delgado-Morales[1*], Victor Contreras Palma[2], Jian Gu[3], and Ernesto Molinas[4]

[1]Institute of Design and Industrial Methods, Universidad Austral de Chile, Chile. E-mail: leonel.delgado@uach.cl
[2]Institute of Naval Architecture and Ocean Engineering, Universidad Austral de Chile, Chile. E-mail: victor.palma@uach.cl
[3]China Ship Scientific Research Center Wuxi, China. E-mail: gujian@cssrc.com.cn
[4]ACQUATOOL Consultoría, Fortaleza, Brazil.E-mail: ernestomolinas@gmail.com
[*]Corresponding author

Abstract

Fatigue can be understood as a process of progressive localized plastic strain that occurs in a material subject to cyclic stresses and strains at high stress concentration locations, whose concentration can cause cracks and culminate in the material's fracture. The fatigue process begins with the appearance of the crack, later on with growth, and finally propagation. The study of this phenomenon can be divided into the function of the material life in low and high cycle fatigue, but some studies address problems in the ultra-low and high number of cycles. This chapter addresses aspects of low cycle fatigue, as it is a relatively unexplored area and for which there are few references. Therefore, the main objective of this text is to describe the main aspects of low cycle fatigue, presenting diverse applications and potential problems in the context of fatigue behavior of materials. For this contribution, a review of the technical literature will be presented, considering relevant publications in the last decade. The text overview considers experimental and numerical aspects, fatigue damage, fracture behavior, thermomechanical fatigue, as well as real cases describing how a low-cycle fatigue problem can be defined and the way to approach it through the use of engineering tools found in the literature. Even though the low-cycle fatigue approach and analysis technique covers all engineering, the purpose of this chapter will be on marine and ocean engineering. Several cases described in the reviewed works will be addressed, where problems related to welded structures, turbines, pipelines, risers, mooring chains, floating systems, and wind platforms are presented, situations related to marine and offshore equipment will also be described, showing how low cycle fatigue can present itself in the various situations above, considering that low-cycle fatigue problems can cause structures to fracture, which could consequently cause serious injuries to life and marine environment. At the end of the chapter, potential applications and problems where this phenomenon can appear will be presented.

Keywords: Low Cycle Fatigue, Review, Potential problems

1 Introduction

In the context of mechanical engineering and the study of material fractures, the assessment of the fatigue phenomenon becomes fundamental. Fatigue can be found in countless situations, from traditional problems of component failures in aircraft, vessels, onshore and offshore systems, civil structures, piping systems and various equipment. Fatigue-related problems can be approached from an experimental or numerical point of view (Beesley et al. [2017]; Han et al. [2018]; Li et al. [2021]), depending on the technological resources and infrastructure available for the study. Fatigue fracture can be produced from mechanical failures, related to the type of loading or for other reasons, such as metallographic defects, temperature effects, corrosion, among others (Sharifi et al. [2016]); Hou et al. [2021]); Lee et al. [2020]; Li et al. [2021]; Jiang and Yang [2020]; Orlando et al. [2021]; Zhang et al. [2021]; Gemilang et al. [2021]).

The fatigue phenomenon can be described as a process of plastic strain, which is located in certain regions of the material and progresses along the rupture surface, when a material is subjected to localized strain and cyclic stresses, with the strain concentration it can cause cracks and culminate in the fracture of the material, requiring the presence of three factors simultaneously: dynamic stresses, tractive stresses and plastic strain (Jia and Ge [2019]). It is possible to affirm that the fatigue process starts with the appearance of the crack (onset or nucleation), later on it propagates (appearance of typical marks â beach lines) and finally the rupture. In general, the study of this phenomenon can be divided as a function of material life in low and high cycle fatigue.

The main motivation for the production of this work is to be able to gather scientific contributions related to low cycle fatigue in a concentrated way, material that can become a source of research for students and researchers interested in the subject. The identification of phenomena related to fatigue problems in naval structures, naval systems and artifacts, equipment, among others, as well as the description of how to approach the problems and all this described in a single text, was also an inspiration and a challenge for the authors.

The pricipal objective of the text is to carry out a literature review, describing the state of the art in the context of studies related to low cycle fatigue, which have been published in recent decades in high-impact scientific vehicles. Identifying applications from different areas of knowledge, experimental and numerical methodologies as well as procedures are also objectives of this chapter.

The bibliographical research is based on an exploratory search, in which works published from the 2010s until the present time were considered, the articles have been resumed in Table 1, which address different aspects and applications where low cycle fatigue is present. The research sources are mostly scientific articles published in highly relevant scientific journals that address topics related to: welded join, risers problems and wind turbines, among others. The texts were analyzed chronologically, making a description of their contents, identifying the main aspects, mainly methodological aspects, technical support and laboratory infrastructure (in the case of experimental work), techniques and procedures adopted, as well as the results obtained. An item was also structured with a description of potential problems which can be addressed through the use of low cycle fatigue.

As a final product, a friendly text was obtained, which addresses the issues in a clear and direct way, based on friendly writing, maintaining scientific rigor. This text can become a source of research for students and researchers, especially those starting in this area of knowledge and who need to find information related to the topic in a concentrated way in a single source.

2 Research related to Low Cycle Fatigue - LCF

Research on Low Cycle Fatigue (LCF) focuses on works done from 2010 until the present. Since the topic of fatigue encompasses a vast number of cases, the specific objective of this book is related to the phenomenon presented only in naval structures and systems. We can distinguish different types of research in LCF, some of the most characteristic are described below:

Ligaj and Szala [2012] proposed calculation formulas in high and low cycle ranges of different metal alloys, those formulations consist of three methods expressed from stress, strain and a hybrid method (Stress-strain). They performed comparative analyzes of C45 steel, using loading programs; two-level and multi-level. The problems analyzed by the researchers finds applications on the analysis of naval structures and increases the ranges of analysis methods found in the previous literature.

Wahab et al. [2013], proposed the use of Continuum Damage Mechanics (CDM) theory for the analysis of high and low cycle fatigue. Then they apply this theory to a simple case such as two plates joined using resin and to a friction fatigue problem, those problems were modeled in ANSYS with the objective of predicting the fracture initiation time. The low cycle fatigue initiation model is based on accumulation of plastic deformation, while for high cycle it is based on the release of energy by plastic deformation.

Benoit et al. [2014] presented an experimental system that includes the effect of temperature at the beginning of the fatigue fracture in low cycle problems, the analysis uses stainless steel as material containing 18% Cr and welded test bodies. The study is used image correlation analysis to obtain the deformation gradient of the test bodies. The analysis of the results were complemented with the use of finite element analysis tools and observation of the fractured surfaces. Finally, they proposed an energy model of micro-fracture growth.

Sharifi et al. [2016] presented a three-dimensional analysis of a low cycle problem found in the cylinder head of an internal combustion engine, the fracture initiatives in the accommodation of the intake and exhaust valves. The study focuses on simulating the durability tests of the failed component, as well as the evaluation of the fatigue of low cycle.The analyses consider five operating speeds of the engine, 750, 1650, 2075, 2350 and 2600 rpm. The cylinder head is exposed to multi-axial cyclic loads. Low cycle failure theories such as critical plane theory and accumulated damage are used to predict the fatigue. Numerical models corroborated that the problem can be analyzed as an LCF phenomenon. The analyses founded that the sector where the valves are accommodated to the cylinder head, which are exposed to high temperatures during engine operation, are the critical areas prompt to LCF.

Amirinia and Sungmoon Jung [2017] studied the buffeting response from three hurricane turbulence models which generated LCF damage in turbine tip blade and tower, this work is described in section four. Hamidi Ghaleh Jigh et al. [2019] studied an aluminum foam subjected to compression by means of the finite element method using representative volumetric elements, together with the above, a series of experiments were carried out applying static loads that caused localized plastic deformation, which leads to low cycle fatigue. This made possible to develop an algorithm that calculate the low cycle fatigue models. The material used was aluminum AA6101-T6, the static load experiments were carried out according to the ISO 13314 standards. The numerical results were compared with the experimental results.

Lee et al. [2020] worked on the study of LCF in offshore oil pipelines caused by external loads. Most of the damage in pipelines occurs in the weld bands, where are presented geometric discontinuities. Along with this, external offshore loads such as currents, swells, and platform movements can cause significant plastic deformation and fractures in a low cycle fatigue regime. ASME 2007 Div. 2 adopts S - N curve for joint fatigue evaluation, in this work were carried out an extension methodology of the S - N curve to evaluate the LCF. However, there is a limitation when describing the behavior of materials when they leave the elastic range of the material because most of the materials in engineering exhibit hardening or softening when subjected to cyclical loads. In this work, they propose an optimized prediction method which was validated with real fatigue data obtained from welds belonging to pipelines used in the industry. It should be noted that this book presents a new problem that could generate Low cycle Fatigue in this type of structure.

Gemilang et al. [2021] studied fatigue phenomenon in anchor chains of offshore platforms, the authors proposed that the traditional system of *S* - *N* curves does not really predict the fatigue life behavior of these chains. In this way, they propose a fatigue criterion based on critical multiaxial planes for anchoring chains that considers the damage produced by cyclical plasticization and medium load effects. To develop these criteria, they used finite element models of the critical points of the chains to obtain the multiaxial critical plane. The results are correlated by the conventional fatigue curves. As a case study, the simulation of the mooring chains of an FPSO was used, which shows that the effect of medium tension load significantly reduces the fatigue life of the mooring chains, while the effect of plasticity inducing damage is more limited. The fatigue damage using the proposed technique is significantly higher than the traditional approach using the *S* - *N* curves.

There are more complex systems to be analyzed in the naval area, this is the case of offshore wind turbines, as the case analyzed by Xu et al. [2021], which studied the bearing system to support the Nacelle of a 5MW offshore wind turbine, these systems are subjected to aerodynamic and hydrodynamic loads at the same time. Load analysis used time domain series of velocity values to establish the loads for which this component is subjected in an offshore wind turbine, various algorithms (Gumbel's algorithm, rainflow counting algorithm and *S* - *N* curves) are used to generate fatigue life load damage. To complete the study, he compared these loads for six types of supports: Onshore, monopile, ITI System(details about this system can be found in Jonkman and Matha [2011]), Tension Leg Platform (TLP), Spar and Semi-submersible. The results of the study show that the dynamics of the wind turbine is directly related to the bearing that allows the Yaw movement of the Nacelle and also that the subcomponents must be taken into consideration for this type of calculation since they also may present low cycle fatigue problems.Another problem present in naval and offshore systems are probabilistic loads, represented by irregular and / or âstrangeâ waves, for this reason a probabilistic study of low cycle fatigue becomes an interesting problem to be studied.

In Song et al. (2021) CDM combined with the cyclic plasticity model is used to evaluate the Low Cycle Fatigue failure of a 10CrNi3MoV steel and its undermached welding. Numerical analysis using the finite element method and supported by ABAQUS is performed. The results make it possible to estimate the fatigue life for both the base material and the undermached welding.

The work of Jiang et al. [2022] presents a model of low cycle fatigue life (ProbLCF-VA), to describe the dispersion of the initiation of fractures by LCF in homogeneous materials subjected to cyclic or random loads. This model can be implemented to estimate probabilistic cumulative damage for a given load history consisting of variable cyclical loads, or to predict the probabilistic onset of the LCF crack, if distributional estimate of a random load spectrum are available. The proposed model describes certain predominant effects such as the interaction of loads and the contributions of small cycles, which are very commonly observed in fatigue tests with cyclic loads of variable amplitude but which can hardly be described by other models with physical and mathematical fundaments.

As well as the previous cases there are other studies that illustrate low cycle fatigue, the following table aims to classify the different types of approaches of the studies in LCF to date (See Table 1).

Table 1: Description of revised works

Author	Year	Research type	Material	Experimental Loads involved in Study
Ligaj and Szala [2012]	2012	Analytical	C45 Steel	-
Wahab et al. [2013]	2013	Analytical - FEA	-	-
Benoit et al. [2014]	2014	Experimental	18% Cr Steel	Thermal and mechanical
Sharifi et al. [2016]	2016	Analytical - FEA	-	-
Beesley et al. [2017]	2017	Experimental	18% Cr Steel	Thermal and mechanical
Amirinia and Sung-moon Jung [2017]	2017	Analytical	Structural Components(Composite fiberglass materials)	Mechanical
Cahís et al. [2018]	2018	Analytical - FEA - Experimental	PC-r5, PC-r45 Steels	Mechanical
Hamidi Ghaleh Jigh et al. [2019]	2019	FEA - Experimental	PC-r5, PC-r45 Steels	Mechanical
Jiang and Yang [2020]	2020	Experimental	AH32 steel	Mechanical
Lee et al. [2020]	2020	Analytical - Experimental	API 5L X65 pipeline Steel-Sainless Steel 304	Mechanical
Zhang et al. [2021]	2021	Experimental	Steel with JQMG50-6 welding wire	Mechanical
Xu et al. [2021]	2021	Analytical - FEA	QT-800	Dynamical Aero/Hydrodynamic
Shaohu et al. [2021]	2021	Analytical - FEA - Experimental	PC-r5, PC-r45 Steels	Mechanical Internal pressure and bending
Orlando et al. [2021]	2021	FEM-Experimental-Time domain measurement	-	Dynamical, non-stationary and stationary
Gemilang et al. [2021]	2021	Experimental - FEA	R4 steel grade for simulation	Dynamical, hydrodynamic
Song et al. [2021]	2021	Experimental - FEA	10CrNi3MoV steel and its undermatched weldments	Mechanical
Hou et al. [2021]	2021	Experimental	K4750 Ni-Based superalloy	Thermo Mechanical
Jiang et al. [2022]	2022	Analytical	-	Mechanical

3 Fundamental concepts and categories of fatigue

Situations involving fatigue are highly complex and require a deep understanding of the cause of the failure, in the case of naval artefacts and offshore structures, other variables appear that make the problem even more difficult to be addressed. One way to predict fatigue failure is to carry out the life estimate while still designing mechanisms or components. The main methods of studying fatigue are the stress life method (S - N) and the strain life method ($\varepsilon - N$). A brief description of these methods is provided below. The stress life method is the oldest and most used, indicated for high cycle fatigue where the deformation is predominantly elastic. It is based on the stress curve versus the number of cycles of the component, considering the fatigue life to total failure. In general is used the Basquin equation for description of fatigue life. (Equation 1) Cui [2002]

$$\sigma_a = \frac{E \cdot \Delta\varepsilon_e}{2} = \sigma'_f \cdot (2N_f)^b, \tag{1}$$

where *E* represent Young's modulus, $\Delta\varepsilon_e$ is the elastic strain, σ'_f is the fatigue strength coefficient, *N* is the number cycles to failure, *b* is the fatigue strength exponent.
J. Kohout [2001] proposed an expression to describe fatigue for low and high number of cycles, the function has the following form (Correia et al. [2017]):

$$\sigma = \sigma_\infty \left[\frac{N + \mathbf{B}}{N + \mathbf{C}}\right]^b, \tag{2}$$

where *a* and *b* are Basquin paranmeters, σ_∞ is the fatigue limit, **B** (Equation 4) is the number of cycles corresponding to the intersection of the tangent line of the finite life region and the horizontal asymptote of the ultimate tensile strength, and **C** (Equation 5) is the number of cycles corresponding to the intersection of the tangent line of the finite life region and the horizontal asymptote of the fatigue limit Correia et al. [2017]. An equivalent equation when considering the ultimate tensile (σ_1 strength) is:

$$\sigma = \sigma_1 \left[\frac{1 + N/\mathbf{B}}{1 + N/\mathbf{C}}\right]^b, \tag{3}$$

$$\mathbf{B} = \beta \cdot \mathbf{C}, \tag{4}$$

$$\mathbf{C} = 10^7 \cdot \frac{1-\alpha}{\alpha-\beta}. \tag{5}$$

The expressions for α and β are defined as:

$$\alpha = \left(\frac{\sigma_c}{\sigma_\infty}\right)^{1/b}, \tag{6}$$

$$\beta = \left(\frac{\sigma_1}{\sigma_\infty}\right)^{1/b}, \tag{7}$$

where is σ_c is the fatigue limit for a pre-defined number of cycles (10^7).
On the other hand, the strain life method is more complex, indicated for low and high cycle fatigue, with plastic and elastic strains. It is based on the strain life curve by the number of cycles of the component, considering the fatigue life until crack nucleation. The contributions of elastic and plastic strains are shown in the following equations:

$$\frac{\Delta\varepsilon_e}{2} = \frac{\sigma'_f}{E} \cdot (2N_f)^b, \tag{8}$$

$$\frac{\Delta\varepsilon_p}{2} = \varepsilon'_f \cdot (2N_f)^c. \tag{9}$$

Where $\Delta\varepsilon_e$ is the elastic strain amplitude, ε'_f is the fatigue strength coefficient, E is the elastic modulus, N_f is the number of cycle to failure, $\Delta\varepsilon_p$ is the plastic strain amplitude, ε'_f represents the fatigue ductility coefficient, *b* is the fatigue strength exponent and *c* is the fatigue ductility exponent Correia et al. [2017], Cui [2002].

Combining Equation 8 and 9 and considering the superposition of elastic and plastic resistance, an expression is obtained to estimate life in the high and low cycle ranges:

$$\frac{\Delta\varepsilon_T}{2} = \varepsilon_a = \frac{\Delta\varepsilon_e}{2} + \frac{\Delta\varepsilon_p}{2} = \frac{\sigma'_f}{E} \cdot (2N_f)^b + \varepsilon'_f \cdot (2N_f)^c. \tag{10}$$

When the effects of mean stress or mean strain are included, the following equation is used:

$$\frac{\Delta\varepsilon}{2} = \frac{(\sigma'_f -) \cdot (2N_f)^b}{E} + \varepsilon'_f \cdot (2N_f)^c, \tag{11}$$

where σ_m is the mean stress, being positive for tensile values and negative for compressive values.

3.1 Fatigue failure categories

Fatigue failure found in engineering materials is a direct function of the type of load and conditions under which the phenomenon occurs. Sharma et al. [2020] presents a classification of the types of fatigue failure that happens in materials used in engineering (See Figure 1).

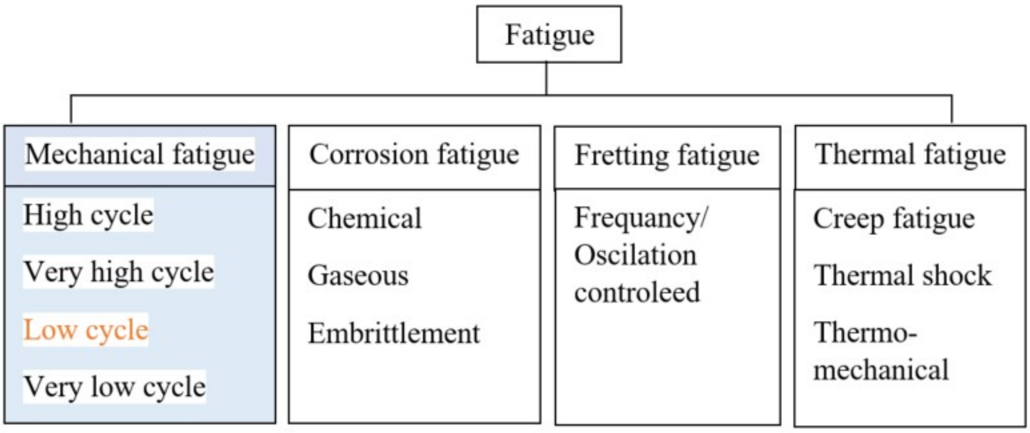

Figure 1: Types of fatigue failure (Adapted from Sharma et al. [2020])

Considering the classification of mechanical fatigue, Neville and Sachs [2020] present three categories, High Cycle Fatigue (HCF), Low Cycle Fatigue (LCF) and Very Low Cycle Fatigue (VLC). A brief description of these categories is given below. The High Cycle Fatigue (HCF) occurs when failure takes more than 10^4 cycles. According to the literature, constituting a significant percentage of all fatigue failures. Components or mechanisms that suffer fatigue failures in this category can take more than 10^5 cycles, in some cases reaching hundreds of millions of cycles from the beginning of application of force to the final failure. Situations in which high cycle fatigue failure occurs are common in several areas of engineering and are widely addressed in the literature. Low Cycle Fatigue (LCF) is when the failure takes less than 10^4 cycles, in general, this type of failure presents itself in a range around 25 cycles from the initial application of force to the final failure. Failures in this category are not very common in industrial equipment, from the point of view of stresses, it can be seen to involve situations in which loads are significantly higher than high cycle failures. Very Low Cycle Fatigue (VLC) occurs less than 10 cycles after charging begins. On the other hand, there are indications that the applied force was slightly less than the force causing the failure. Very High Cycle Fatigue (VHCF) is can be found in situations where the fatigue life is greater than 10^7 cycles. Industrial equipment failures in this category are not very common, however the phenomenon is seen more often than low-cycle fatigue cases. This category has very particular aspects, which differ from HCF and LCF, especially regarding plastic strain levels. The term âinfinite lifeâ is usually used when a component has such a long fatigue life that it will not fail due to this phenomenon. In carbon steels, the number of cycles considered as infinite life must be greater than 10^6. On the other hand, finite life means that the component will fail due to fatigue in a certain number of cycles. Figure 2 shows a schematic figure with the ranges of the categories described.

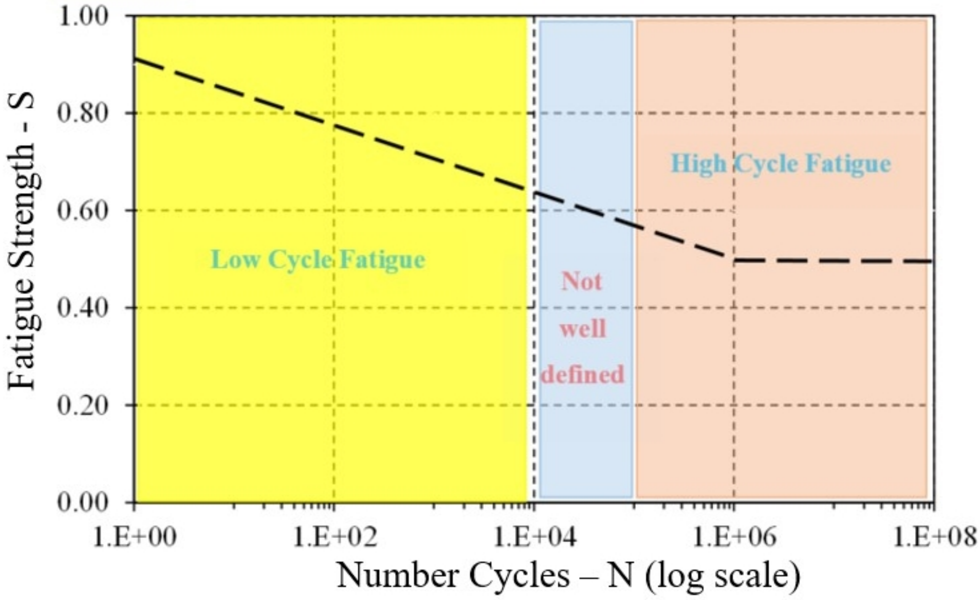

Figure 2: General ranges of fatigue stress cycles (Adapted from Neville and Sachs [2020])

4 Description of Low Cycle Fatigue problems in offshore engineering

This section presents a description of specific jobs in the context of offshore engineering to which low cycle fatigue is applied. The contribution made by Amirinia and Sungmoon Jung [2017] is described, in which the problem of a wind turbine is addressed. Another work described is the publication by Gemilang et al. [2021], where the problem of estimating the life of mooring chains of an FPSO is investigated and finally the paper by Song et al. [2021], where the problem of predicting the life of an undermached welding is studied.

One of the concerns in some structural analyses in LCF are the effect of climate change over offshore structures, specially because the increment of hurricane events in places where offshore wind turbines are installed or future develoment of OWT projects could be implemented. LCF analysis can be evaluated to determine the structural integrity during this extreme events, the work of Amirinia and Sungmoon Jung [2017] adress this issue, where three hurricane turbulence models where considered to describe the energy amount which can affect the turbine during those short periods.

Those wind turbulence spectrums are described as a superposition of eddies. Big eddies, which represent small wave numbers or low frequencies, supply the most energy content of the turbulent flow. In contrast, small eddies with high wave numbers in high frequencies dissipate the gained energy. The three models are:

Kaimal model (Kaimal et al. [1972]):

$$\frac{nS_u}{\sigma_u^2} = \frac{21.6f}{(1+33f)^{5/3}}. \tag{12}$$

Model A:

$$\frac{nS_u}{\sigma_u^2} = \frac{1}{\beta} X \frac{p_1 f^2 + p_2 f + p_3}{f^3 + q_1 f^2 + q_2 f + q_3}. \tag{13}$$

Where $\sqrt{\beta} = \sigma/u^*$is the turbulence radio, u^* represents the friction velocity, and $q_i$and p_i are constants proposed by Yu et al. [2008].

Model B:

$$\frac{nS_u}{\sigma_u^2} = \frac{16.66f}{1.72 + 237.24f^{5/3}}. \quad (14)$$

Where $f = nz/Uz$ is the normalized frequency, n is the frecuency, $S_u$is the spectral density of the longitudinal velocity fluctuation at height z, and σ is the standar deviation of longitudinal velocity fluctuation.

The effect of those models where studied over the structure at the tower and blade of the wind turbine.Buffeting response over the cited components is the main studied effect in this work.

The Buffetting load can be defined as the dynamic amplification of the structural response of the turbulent component of the wind and the impulsive action of periodic gusts (A. Pipinato [2022]).

Wind load on the wing turbine tower is given by:

$$F_{wind(z,t)} = \begin{bmatrix} \vec{f}_{D}(z) \\ \vec{f}_{L}(z) \\ \vec{M}_{a}(z) \end{bmatrix} + \begin{bmatrix} f_{D}(z,t) \\ f_{L}(z,t) \\ M_{a}(z,t) \end{bmatrix} = \vec{f} + B_f v + C_{ac}\dot{r} + K_{ae}r. \quad (15)$$

Where $\vec{f} = [f_D(z,t), f_L(z,t), M_a(z,t)]^T$ are quasi-static forces $B_f v$ are Buffeting forces,$C_{ac}\dot{r}$ and $K_{ae}r$ are self exited forces, u and w are longitudinal and and lateral fluctuating parts of the wind, r and $r\hat{A}$are structural position and velocity vectors.

$$v(z,t) = [u/Uw/U]^T. \quad (16)$$

and

$$\vec{f} = [\vec{f}_D(z), \vec{f}_L(z), \vec{M}_\alpha(z)]^T. \quad (17)$$

The therm $B_f v$ in the Equation 15 denotes the buffeting force and can be expressed as:

$$B_f(z)v(z,t) = \frac{\rho U^2 D}{2}[2X_{Du}\vec{C}_D u(t) + (C_D - \vec{C}_L)X_{Dw}W(\tau)]. \quad (18)$$

Due to wind fluctuations the therms u and w can be expressed as the convolution integrals:

$$B_f(z)v(z,t) = \frac{\rho U^2 D}{2}\int_{-\infty}^{t} I_{Du}(t-\tau)u(\tau) + I_{Dw}(t-\tau)w(\tau)d\tau. \quad (19)$$

Where I_{Du} and I_{Dw} are the aerodynamic impulse functions in along wind and across wind directions respectively. The effects over the tower and blade tip of the three models for different wind speeds can be described in figure 3 A and B, which describes the moments at those sections.

Those moments generated displacements as can seen in figure 4 A and B. With the above information the low cycle fatigue analyses can be adressed, indicating very large loads in a short period.The fatigue load over the structure can be represented as Miners Rule:

$$DI = \sum_{i=1}^{j} \frac{n_i}{N_i}. \quad (20)$$

$$\epsilon_a = \epsilon_{a,e} + \epsilon_{a,p} = \frac{\sigma_f}{E}(2N_f)^b + \epsilon_f(2N_f)^c. \quad (21)$$

Here the equation represents the LCF in the wind turbine steel tower. The LCF can affect the fiberglass material of the blade structure, conventional test-load method and simplified load stress method are the most common fatigue models for blades, the Coffin Mason ϵ-N curve describes the LCF fatigue load during hurrican at 5 A and B for fiberglass.

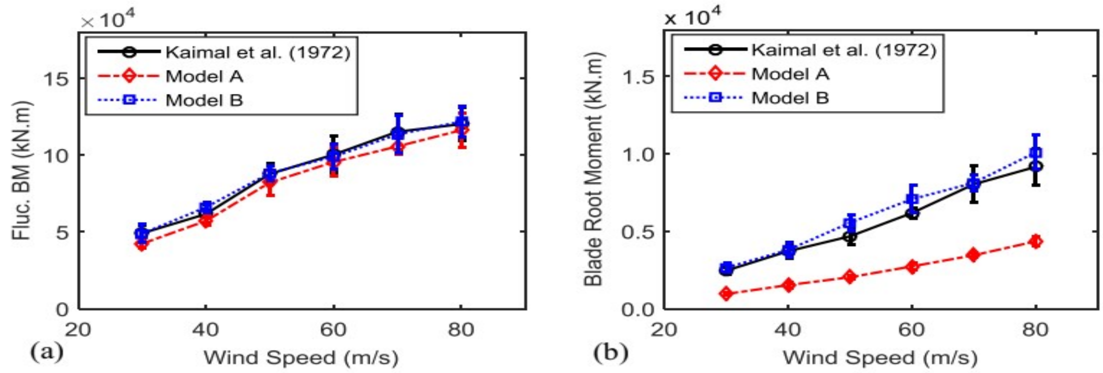

Figure 3: Mean of maximum (a) tower buffeting fore-aft base moments and (b) blade root edge-wise buffeting moment for different wind speeds at 10 m height (Amirinia and Sungmoon Jung [2017])

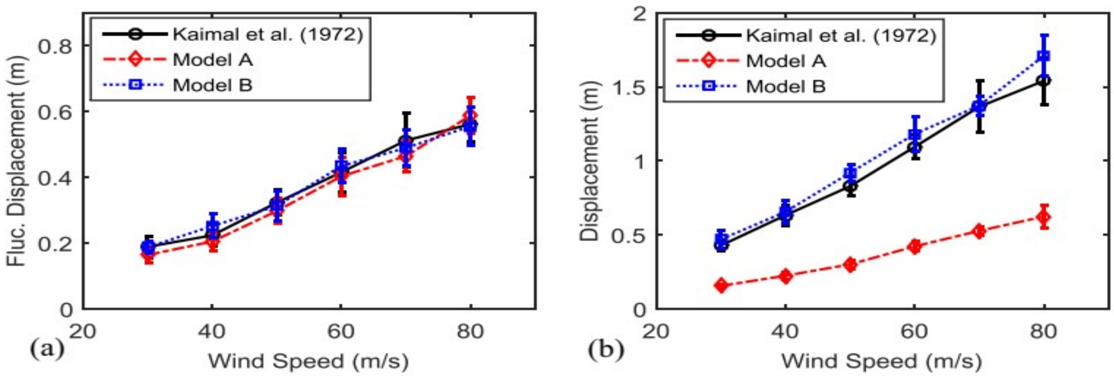

Figure 4: Mean of maximum (a) tower tip buffeting displacements and (b) blade tip displacements for different wind speeds at 10 m height(Amirinia and Sungmoon Jung [2017])

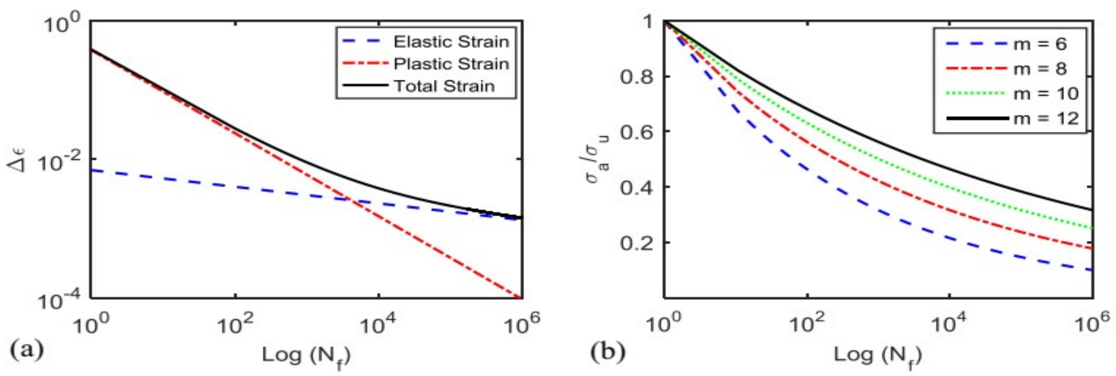

Figure 5: (a) Coffin-Manson ϵ-N curve and (b) fiberglass σ-N curve (Amirinia and Sungmoon Jung [2017])

Since the mean wind speeds and turbulence intensities of various models were identical, the mean load and accordingly the mean damage index caused by fatigue were almost the same; however, different turbulence spectrums resulted in different damage indices in buffeting responses. Authors considered 2 h of hurricane load on the wind farm location, and presented tower base buffeting damage indices, where the spectrums Model A and Model B have average 53% smaller and 12% larger damage indices compared to Kaimal (Kaimal et al. [1972]) models.Also, the authors shows the blade root damage indices for different wind speeds and hurricane categories where spectrum Model A and Model B resulted in 96% smaller and 24% larger damage indices compared to Kaimal (Kaimal et al. [1972]) model.

Finally the authors stated that further Research is needed to address lateral fluctuation components of Model B and investigate the responses such as tower side to side moment, blade flap-wise moments, and damage indices correlated with lateral components.

In Gemilang et al. [2021]) low cycle fatigue is addressed, applied to an offshore mooring chain. In the study, a multiaxial fatigue approach was carried out, since the effects of the stress-strain state are neglected in a traditional approach, as is the case with the (S - N) method. The chain geometry was defined in accordance with the requirements stipulated by the International Association of Classification Societies (IACS), using R4 steel grade material for its manufacture. The numerical solution, using the Finite Element Method (FEM), was carried out with the aid of the commercial software ABAQUS, being modeled the problem in a simplified way, taking advantage of the symmetry presented by the geometry of the chain. The model called Mono-Rampi, based on bilinear isotropic hardening to derive the mechanical properties of the material, is developed. From the model, it is possible to establish a prediction of the elastoplastic behavior of the material, through a stress-strain curve, as shown in the Figure 6.

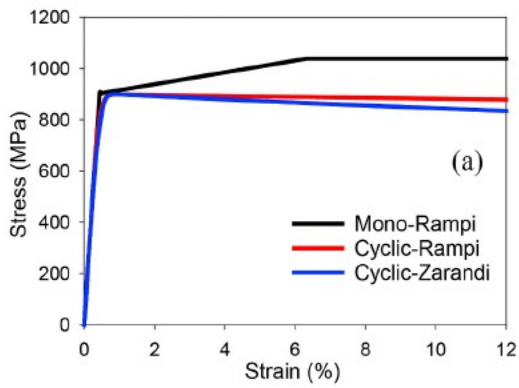

Figure 6: Stress strain curve for bilinear monotonic material model under monotonic loading (Gemilang et al. [2021])

To evaluate the cyclic behavior of the material, the Chaboche constitutive model in linear is used, based on combined isotropic-kinematic hardening, which allows to obtain the behavior of the material for low cycle fatigue. The material response is shown in Figure 7.

To achieve the objectives of the study, the fatigue model based on the critical plane, proposed by Smith-Watson-Topper (SWT) was used. In this method, the fatigue damage is assessed directly in terms of local strains and stresses under progressive loading cycles. The SWT model can be written as follows:

$$SWT = \sigma_{n,max} \frac{\Delta\epsilon_n}{2}, \tag{22}$$

where *SWT* is the damage parameter, $\sigma_{n,max}$ is the maximum normal stress and $\Delta\epsilon_n$ is the normal strain range perpendicular to the critical plane during one cycle.

From Equation 23, a relationship is established which allows estimating the life until failure of the material. The formula based on the SWT model has the following form:

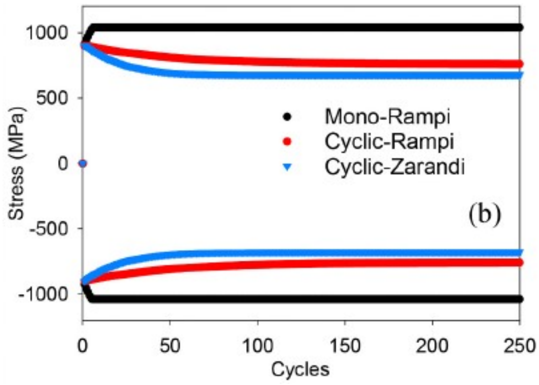

Figure 7: Evolution of the stresses with the number of cycles for Chaboche cyclic material model under cyclic loading (Gemilang et al. [2021])

$$SWT = A_1 N_f^{a_1} + A_2 N_f^{a_2}, \tag{23}$$

where N_f represent the number of cycles to failure, the constants A_1, A_2, a_1, a_2 are material characteristic, determined by calibration tests from experimental data.

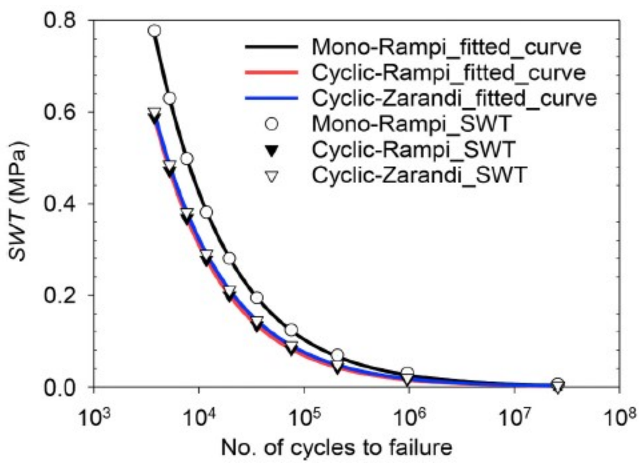

Figure 8: Fatigue life of mooring chains for the SWT (Gemilang et al. [2021])

Gemilang et al. [2021] perform simulations to estimate loads of the mooring line of an FPSO, in a given configuration, for different sea conditions. They make a prediction of low cycle fatigue life, considering the critical plane, the effects of cyclic plasticity and the mean load.

In the work by Song et al. [2021] Continuous Damage Mechanics combined with the cyclic plasticity model is used to evaluate the Low Cycle Fatigue failure of a 10CrNi3MoV steel and its undermached welding. The investigation takes an experimental and numerical approach, using the constitutive Lemaitre-Chaboche model with kinematic hardening. Hysteresis loops are obtained, evaluating the evolution of the maximum and minimum stress, as well as the accumulative plastic strain per cycle for different stress levels obtained. The material used in the investigation was quenched and tempered, and the V-groove joints were fabricated using the Single Pulse Gas Metal Arc (SPGMAW) welding process. Cylindrical specimens were used, which were subjected to a heat treatment to eliminate potential residual stresses. Tests were carried out to estimate the Low Cycle Fatigue (LCF) life, for which an Instro testing machine equipped with strain gauges was used. The commercial program of Finite Element Analysis (FEA) ABAQUS, was used for the numerical analysis, being implemented a routine to describe the yield surface, considering nonlinear isotropic and kinematic hardening. The yield surface can be represented by the following expression:

$$f(\sigma - \alpha) = \sqrt{\frac{3}{2}(S - \alpha^{dev})) : (S - \alpha^{dev})}, \tag{24}$$

where, σ is the stress tensor, α^{dev} is strands for the deviatoric part of the back stress tensor and S is the deviatoric stress tensor.

Song et al. [2021], establish that the evolution of damage, under cyclic loading, can be measured through the variation of the Young's modulus, for this a relationship between elasticity, plasticity and damage is proposed, through the following expressions:

$$D_i = 1 - \frac{E_i}{E'}, \tag{25}$$

where, D_i represents the *i*th cycle, E' is the initial Youngâs modulus, and E_i is the apparent Youngâs modulus of the *i*th cycle.

$$D_i = 1 - \frac{\Delta w_i}{\Delta w_0}, \tag{26}$$

where Δw_i the apparent hysteresis energy density of the *i*th cycle, $\Delta w_0$is the hysteresis energy density after cyclic softening.

The initiation of damage for ductile materials subjected to LCF is related to the cyclic hysteresis energy which can be represented as follows:

$$N_0 = c_1 \cdot \Delta w_0^{c_2}, \tag{27}$$

where N_0 refers to the number of cycles of the damage initiation and Δw_i is the hysteresis energy density of the stabilized cycle. The parameters c_1, c_2 are the material constants, which are fitted from the experimental tests. The linearized Equation 27 can be written as:

$$log(N_0) = c_2 log(\Delta w_0) + log(c_1), \tag{28}$$

here, N_0 stands for the numbers of the cycle before hysteresis loop stabilization according to experimental data.

Another important aspect to be described is the damage evolution, in this study a relationship based on the plastic hysteresis energy density is proposed, represented by the following equation:

$$\frac{dD}{dN} = \frac{c_3 \Delta w^{c_4}}{L}, \tag{29}$$

where Δw is the average of the plastic hysteresis energy density of the stabilized cycle. The constants c_3 and c_4 represent the material properties. L is the characteristic length associated with an integration point.

Analogously to the initiation of damage, it is possible to obtain the parameters c_3 and c_4, through the following expression:

$$log(N_e) = log(\frac{L}{c_3}\Delta D) - c_4 log(\Delta w). \tag{30}$$

After obtaining the constants c_3 and c_4, by means of a curve fitting, it is possible to obtain a final fatigue life equation

$$N_f = c_1 \cdot \Delta w_0^{c_2} + \frac{L}{c_3 \cdot \Delta w^{c_4}} \cdot \frac{1}{(1 - c_4)}. \tag{31}$$

The comparisons of the experimental and numerical results of the first hysteresis cyclic stressâstrain curves of 0.6% and 0.8% are shown in Figure 9 for the metal base and Figure 10 for undermatched welds. The stable hysteresis loop at half-life cycle from the strain range from 0.6% to 1.2% for base metal and weldments is presented in Figure 11. The fatigue life prediction performed by Song et al. [2021] can be seen in the Figure 12.

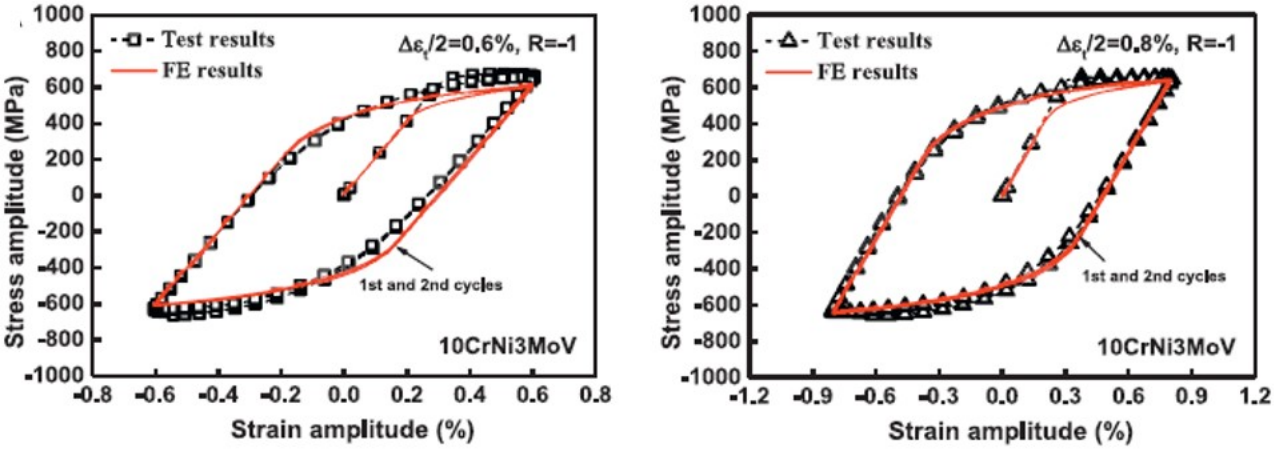

Figure 9: Experimental and simulation comparisons for metal base (10CrNi3MoV steel) (Adapted from Song et al. [2021])

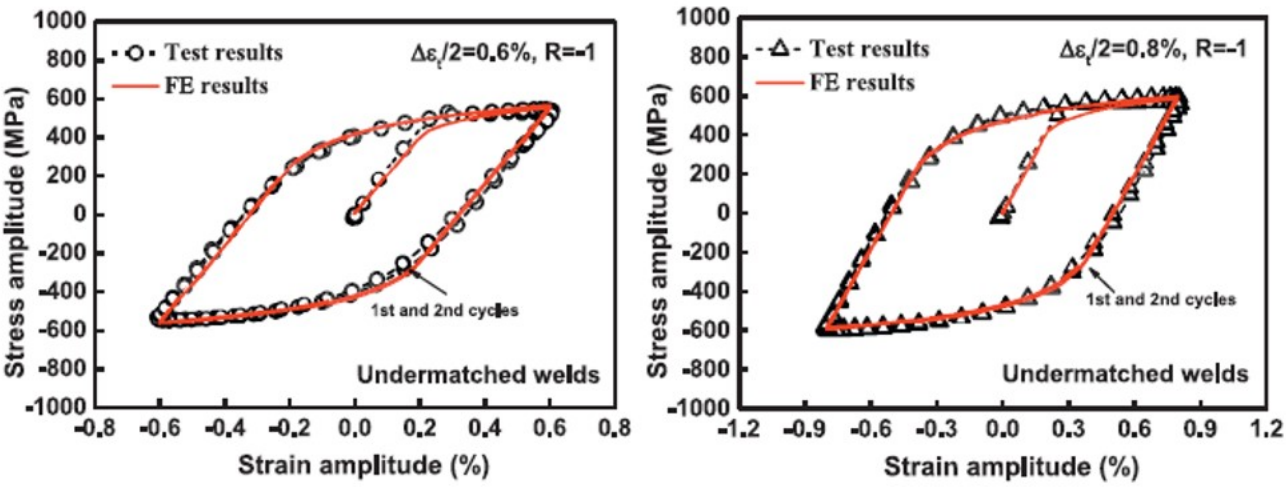

Figure 10: Experimental and simulation comparisons for undermatched welds (Adapted from Song et al. [2021])

5 Identification of new potential problems in Low Cycle Fatigue

One of the main purposes of this review is search for novel problems related to LCF in Ocean Engineering, two cases are described above, this work doesn't intend to give a solution, the authors are working in the analyses of those issues and pretend to give more details in future works.

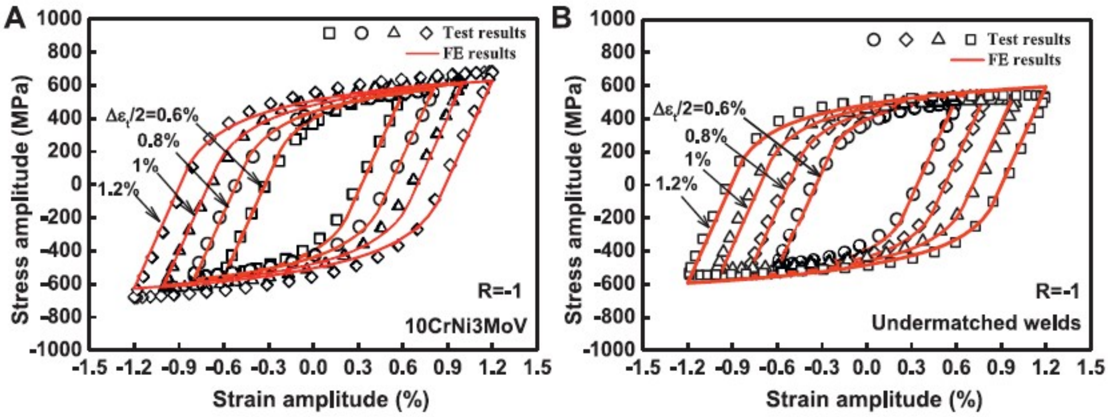

Figure 11: Experimental data and simulation results of hysteresis loops at the half-life cycle for specimens (Adapted from Song et al. [2021])

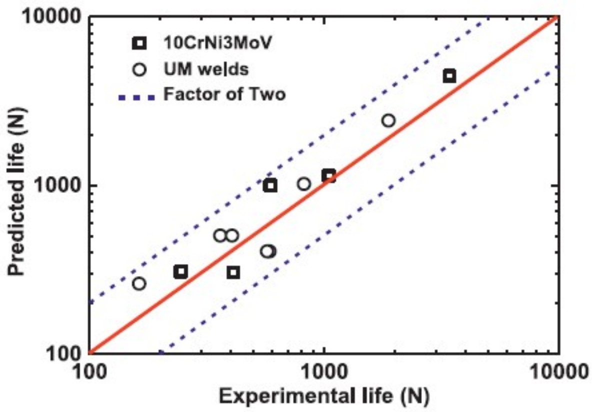

Figure 12: Fatigue life prediction of different materials (Adapted from Song et al. [2021])

5.1 Problem for an Offshore structure: Internal Oceanic Waves (IOW)

The potential problems associated to LCF in offshore systems are intrinsically dependent on the characteristics of oceanic environment forcings. In this context, (IOW) represent the most energetic high-frequency event in coastal oceans, as well as in ocean basins. The amplitude of typical IOWs can reach tens of meters, acting as an important generation mechanism for currents and turbulence (Pomar et al. [2012]). The IOWs develop in the density gradient of the permanent thermocline, the lower limit of the oceanic mixture layer.

The main generating mechanism of these waves is the tidal current excitation over the deep oceanâs density structure. For this reason, they are commonly called internal tides (Apel et al. [1995]). Oceanic thermoclines occur at varying depths (usually between 20 and 600 m), with density gradients of the order of 10^{-2} to 10^{-3} $kg/m^3/m$, generating Brunt-Väisälä periods of the order of 100 to 300 s. The combination of high fundamental periods with low vertical velocity gradients means that the Richardson numbers of these environments can frequently exceed the unit by far.

The interactions between the moving thermocline and the topographic irregularities of the continental shelf can cause resonant effects or the eventual break of internal tides. This gives rise to another type of oscillatory phenomenon, with frequencies close to those of Brunt-Väisälä waves, so-called internal solitary waves (ISWs). ISWs are characterized by being nonsinusoidal and nonlinear and by presenting themselves in the form of isolated groups of complex shape, generated periodically according to the internal tides. These groups generally present 3 to 12 ISWs with decreasing amplitudes (Apel [2002]), as descripted in Figure 13. Garrett and Munk [1979] provide an extensive review of the physical properties of internal oceanic waves.

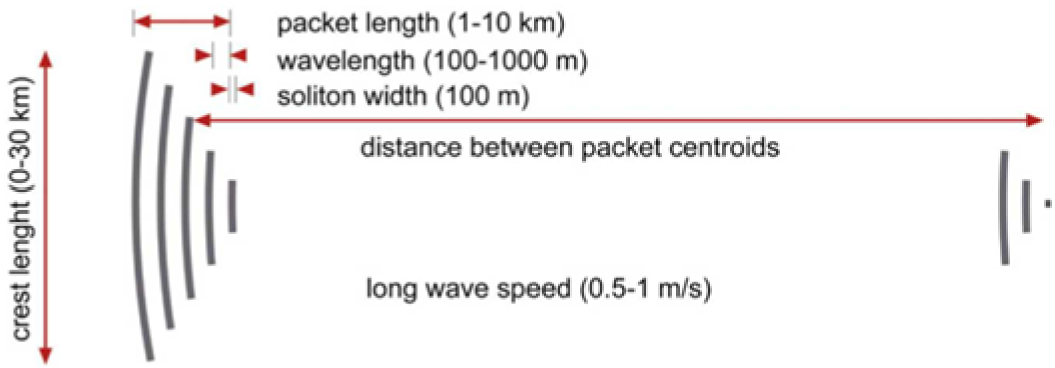

Figure 13: Typical horizontal dimensions associated to the groups of ISWS (Apel [2002])

Unlike internal tides, ISWs generate short waves (wavelengths varying from 102 to 103 m) that sharply alter the free-surface roughness, allowing their detection by Synthetic Aperture Radar (SAR) satellite images. In Figure 14 Jackson and Apel [2004] illustrate how widely distributed this phenomenon is, being especially relevant in regions where the existence of expressive astronomical tides and extensive continental shelfs are combined.

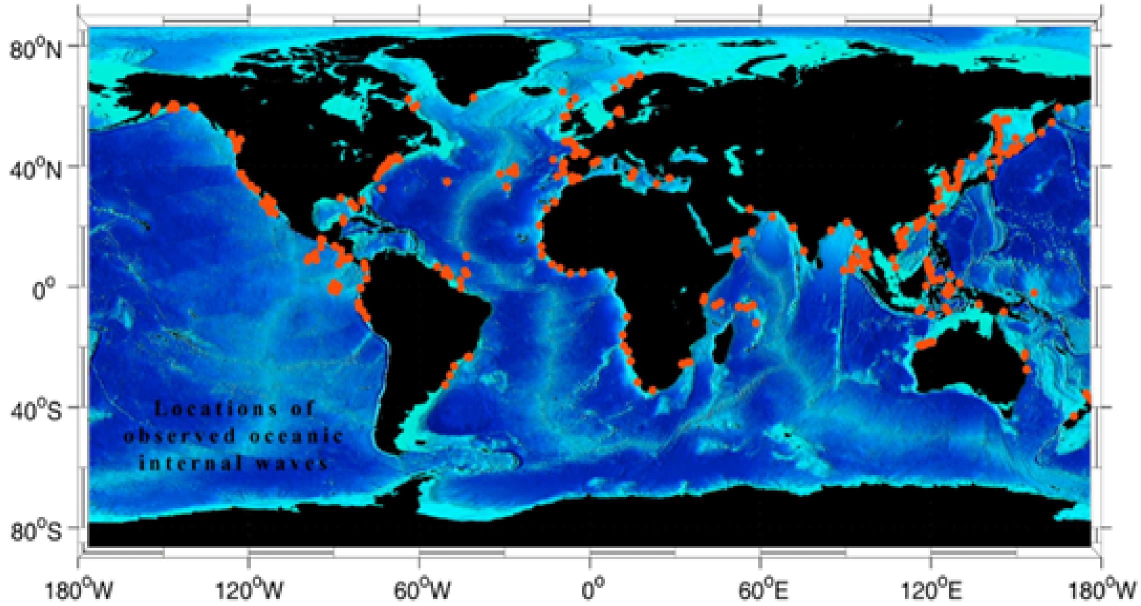

Figure 14: Localization of observed OIW and ISW making use of SAR satellite images(Jackson and Apel [2004])

In the sense of achieving a better understanding about the formation and propagation of ISWs packets, as well as to describe its vertical velocity structure, computational fluid dynamics technics represent a powerful tool. Figures 15 were obtained using a set of computational models developed under the Delft3D platform in the works of Molinas [2020] and Molinas et al. [2020] and represent a hypothetical situation that resembles the typical characteristics of the ISWs packets that are formed on the Amazon continental shelf (a worldwide hotspot for this phenomenon). Figure 15 (panel A) illustrates the surface signature of two consecutive ISWs packets moving away from their formation zone in the shelf break (propagation to the right). The panel B of the same figure highlights the crests and troughs of the nine ISW that form the packet to the left in the panel A.

Figure 16 shows the vertical structure of the horizontal currents associated to the passage of one these ISWs packets. In comparison with Figure 15, it is important to notice that every water surface crest in Figure 15 corresponds to a thermocline trough in Figure 16 (black lines represent isopicnal surfaces). Antagonistic behaviors occur above and below the pycnocline.

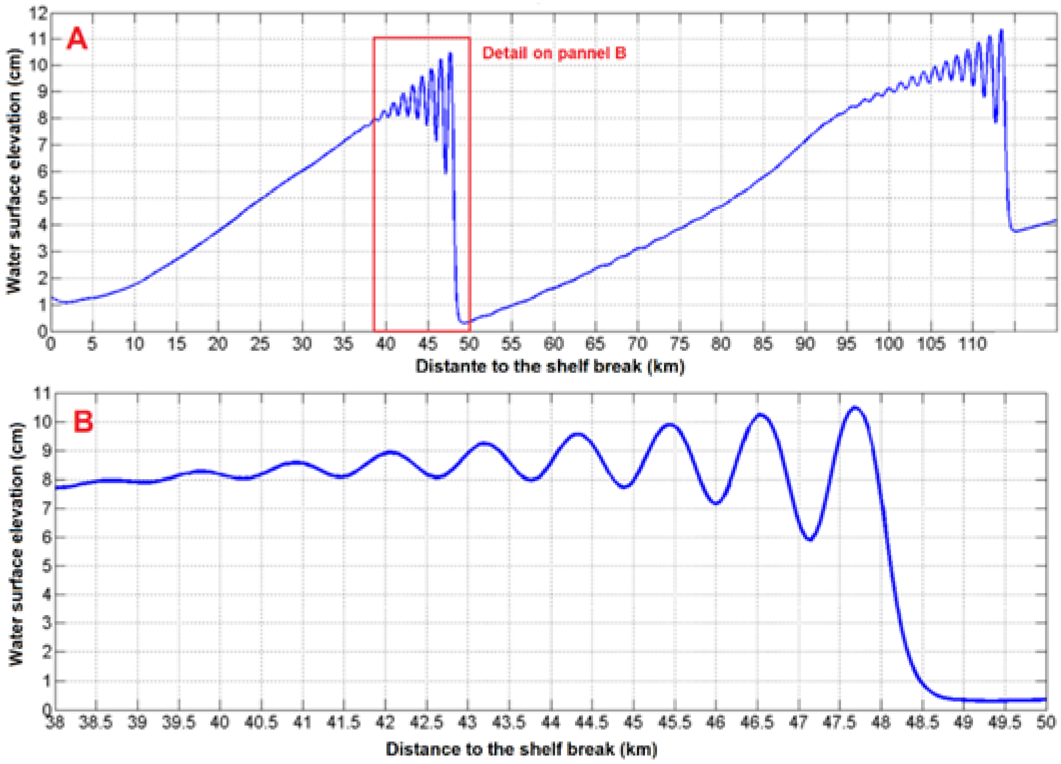

Figure 15: Surface signature of the passage of two consecutive ISWS packets (Molinas [2020] and Molinas Molinas et al. [2020])

In the upper layer (0 to 140 m depth), water surface crests (pycnocline troughs) correspond to regions where the horizontal currents achieve their maximum velocities (up to 40 cm/s in the first wave of the packet), coinciding with the direction of wave propagation. Water surface troughs (pycnocline crests), for instance, represent regions of minimum velocities, still in the direction of wave propagation but with intensities below 10 cm/s.

In the bottom layer (140 to at least 600 m depth), water surface crests (pycnocline troughs) correspond to regions of minimum horizontal currents, achieving values of -10 cm/s, thus in the opposite direction of wave propagation. Water surface troughs (pycnocline crests), for instance, represent regions of local maximum velocities, still in the direction of wave propagation but with intensities in the order of 10 cm/s.

This complex 2DV patterns of oscillatory horizontal velocities area capable of generating major load on structures, especially in what concerns LCF, in the case of risers, flexibles, and mooring systems those waves can potentially produce phenomenon associated to Vortex Induced Vibration (VIV). In general, what we expect is the generation of nearly 10 cycles per semidiurnal

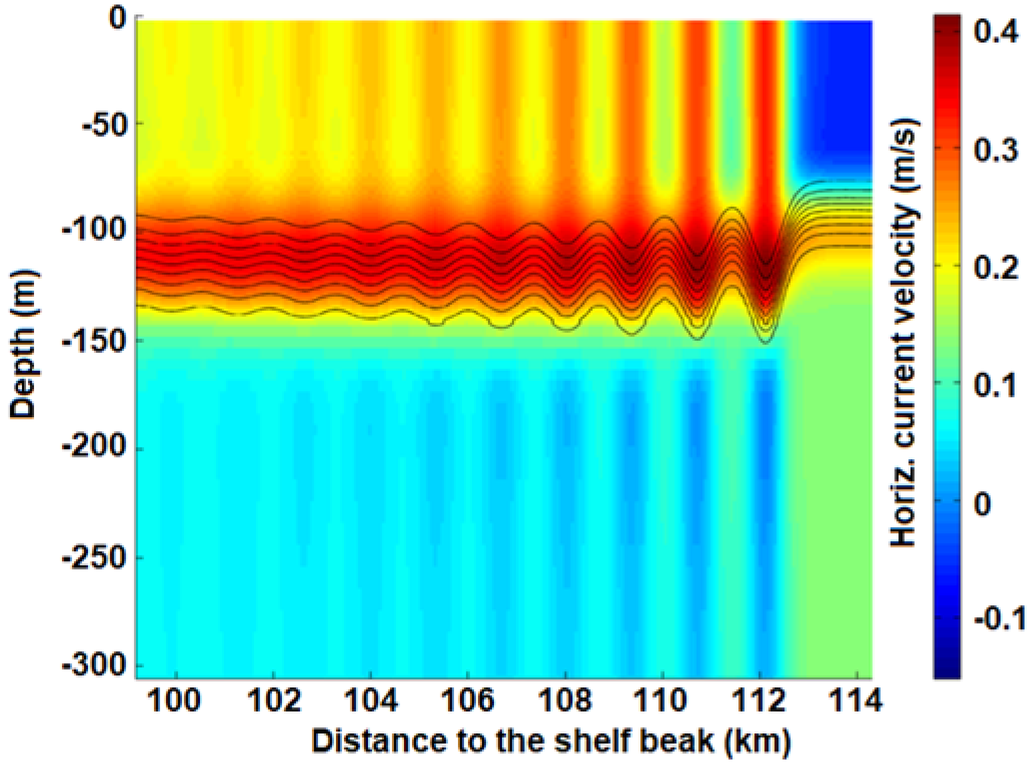

Figure 16: 2DV structure of the horizontal current velocities associated to the passage of a ISWS packet (Molinas [2020] and Molinas et al. [2020]).

tide, what would represent a basis of 7,300 cycles per year or more than 200,000 cycles if we consider a 30-year lifetime for a structure.

5.2 Problem for an Offshore structure: fatigue damage at the touchdown

In ocean engineering, various risers are crucial in the oil and gas (O&G) production systems, conveying the multi-phase flows from the seabed to the floating platform. As a result, the marine risers often need to suffer from complex excitations, including the wave-frequency (WF) responses and low-frequency (LF) drift of the vessel, vortex-induced motion (VIM), and VIV. In addition, the seabed and internal flows could also impact the behavior of the riser. Therefore, there would be plenty of sources for fatigue damage of risers. The fatigue damage at the touchdown zone (TDZ) of the steel catenary riser (SCR) is critical and has recently been paid much attention.

As the O&G exploitation steps into deeper water, the application of SCR becomes wider due to its excellent combined performances of reliability and economy. However, as illustrated in Figure 16, the touchdown point (TDP) between the riser and seabed is found to be more susceptible to appear stress concentration which leads to fatigue damage. According to the subsea survey by remote operating vehicles (ROV), the trench will be generated beneath the SCR with a depth of several riser diameters due to the riser-soil interaction.

Langner Langner [2003] investigated this self-trenching phenomenon of an SCR at the TDP of soft seafloor. By comparing the fatigue damages with rigid seafloor, the curved trench was found to reduce the fatigue risk at the TDP. The riser-soil interaction model, Randolph and Quiggin [2009] proposed a non-linear hyperbolic function to model the seabed resistance forces due to the penetration. With such a function, the high stiffness on reversal forces due to the small cyclic displacements, and the asymptotic behavior with limiting penetration and uplift resistance, can be captured in the analysis of riser-soil interaction.

To deal with the conventional linear soil model, Hejazi and Kimiaei [2016] introduced the âequivalent linear soil stiffnessâ instead of the complex and time-consuming nonlinear riser-soil interaction model. The stress ranges corresponding to different SCRs were compared between the proposed linear soil model with equivalent stiffness and the nonlinear soil model. A simplified hyperbolic formulation of the equivalent linear stiffness was provided, which was noted insufficient in considering abundant geometrical parameters, irregular motions at different sea states, and trench formation. To improve the efficiency, Qu [2015] proposed a simplified approach to deduce the dynamic responses of the SCR by the dynamic amplification factors (DAFs). Meanwhile, the performance of this approach was found dependent on the fitness of DAF evaluation. Therefore, sensitivity studies were conducted to provide quantitative guidance in estimating DAFs and other parameters.

In view of the limitations of linear riser-soil interaction (RSI) model, many research determined to develop the nonlinear RSI model. Wang et al. (Song et al. [2021], Wang et al. [2013]) introduced a TDZ element into the riser-soil interaction simulation to improve the accuracy of the fatigue analysis at the TDZ.

The influences of seabed stiffness, soil suction forces, mudline shear strength and trench depth were investigated on the fatigue damage, applying the linear hysteretic riser-soil interaction model with TDZ element. As a result, the large seabed stiffness and mudline shear were found harm to the fatigue life of the SCR, while the large soil suction and trench depth were found in favor of the fatigue life. Later, Wang et al. [2013] conducted a large-scale model test of a truncated SCR, where the two-dimensional (2D) in plane motion was imposed at the upper truncated point of the SCR and its impacts on the fatigue damage were investigated.

In the tests, both the in-plane and out-of-plane VIV was induced by the 2D motion, while their influences on the fatigue damage were found dependent on the amplitude and period of the motion. Three critical locations of maximum fatigue damage were concluded by the model tests, namely the TDP, upper sag-bend and top of the SCR.

Similarly, Yuan et al. [2021]carried out experiments to investigate the riser-soil interaction at the TDZ, considering the VIV of the SCR. Both the length and depth of the trench was shown to enlarge with severe heave excitation, while the heave level had less influence on the trench location. Meantime, the VIV was exhibited to make the trench depth growing more smoothly. To predict the fatigue damage of SCR coupling with in-line (IL) and cross-flow (CF) VIV, Wang et al. [2014] further established a time domain approach based on the Euler-Bernoulli equation with empirical hydrodynamic coefficients input.

The previous mentioned (Wang et al. [2015]) riser-soil interaction model was adopted in the simulations which investigated the effects of IL and CF VIV on the fatigue damage of the SCR along the TDZ. Regarding the impacts of trench formation on fatigue damage in the TDZ, Shiri [2014] revealed that the final fatigue damage was independent on the order of the applied waves and the number of the applied wave cycles, given initially created trench. Also, the peak fatigue damage was no longer controlled by the maximum shear force once a trench was created initially.

Substantially, the fatigue of SCR is caused by the cyclic elastic-plastic-damage of the structure. To investigate the constitutive behavior of a next-generation SCR material, i.e. X100Q, Devaney et al. [2018] employed experimental and numerical methods, respectively, which captured the two-stage fatigue damages, namely the early-stage microcracking damage and the secondary damage accumulation. Integrating the low-Cycle fatigue (LCF) and high-Cycle fatigue (HCF) models, the effects of strain range on the damage evolution was predicted successfully.

Also, the interdependency was revealed between the material degradation induced by fatigue damage and the cyclic plasticity at the weld for a range of load cases. To clarify the influences of trench on fatigue damage at the TDP, Shoghi and Shiri [2019] investigated the dependency of fatigue damage on the variable TDZ in the trench, due to the low-frequency drift of the vessel using both analytical and numerical approaches. The peak fatigue damage was found decreased in the far offset zone (FOZ), while increased in the near offset zone (NOZ), as illustrated in Figure 17.

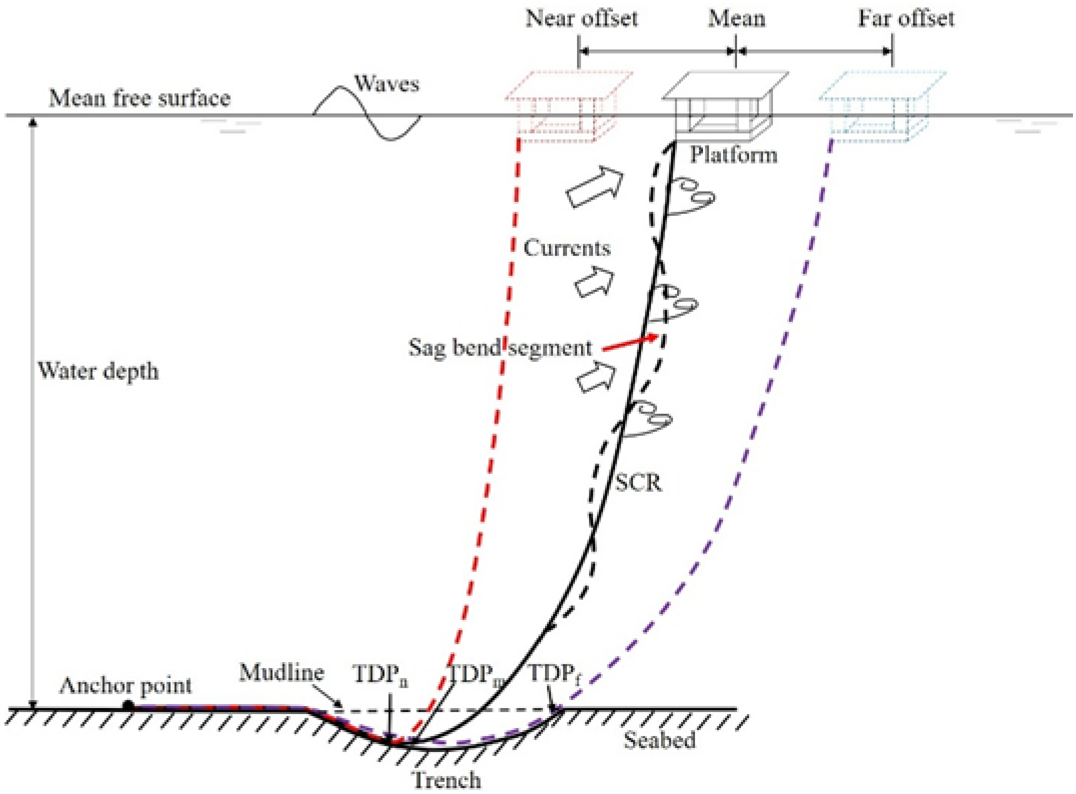

Figure 17: The schematic view of the SCR considering soil-riser interaction

Also, the fatigue damage variation due to the trench effect was found dependent on the direction of the predominant fatigue sea states and the low-frequency excursion of the vessel.

6 Concluding Remarks

This chapter presents an updated compilation of works related to Low Cycle Fatigue and its application in the context of naval and offshore engineering. A series of contributions published in important scientific journals and relevant congress proceedings were described. The text was structured in a friendly way and an easy-to-understand language so that it can contribute, especially for researchers who wish to start studies in the context of Low Cycle Fatigue. Furthermore, a review of theoretical aspects was carried out, fundamentally softening numerical and experimental aspects. The identification of potential problems related to Low Cycle Fatigue, in the context of offshore structures, were presented, in order to encourage the investigation and approach of these and other issues related to the main theme of the text.

Fatigue failure of marine structures can cause catastrophic social,environmental, and economic damage. Studying novel problems related to LCF in naval and offshore structures can avoid potential accidents and improve safety in those systems. Future works aim to study the potential of IOWs effects on naval and offshore structures, especially risers, umbilical, and mooring systems.

Acknowledgements

The authors gratefully acknowledge the Faculty of Sciences of Engineering - Universidad Austral de Chile, China Ship Scientific Research Center Wuxi and ACQUATOOL Consultoría for their support and encouragement for this publication.

References

A. Pipinato. *Innovative Bridge Design Handbook*. Elsevier, 2nd editio edition, 2022. ISBN 9780128235508.

G. Amirinia and Sungmoon Jung. Buffeting response analysis of offshore wind turbines subjected to hurricanes. *Ocean Engineering*, 141(April):1–11, 2017. ISSN 00298018. doi: 10.1016/j.oceaneng.2017.06.005.

J. Apel. *Atlas of Oceanic Internal Solitary Waves*. 2002.

J. Apel, Ostrovsky, S. L.A., and Y.A. Internal solitons in the ocean. The Journal of the Acoustical Society of America 98. *The Journal of the Acoustical Society of America*, 98(2863â2864), 1995.

R. Beesley, H. Chen, and M. Hughes. A novel simulation for the design of a low cycle fatigue experimental testing programme. *Computers and Structures*, 178:105–118, 2017. ISSN 00457949. doi: 10.1016/j.compstruc.2016.09.004. URL `http://dx.doi.org/10.1016/j.compstruc.2016.09.004`.

A. Benoit, L. Rémy, A. Köster, H. Maitournam, and F. Oger. Experimental investigation of the behavior and the low cycle fatigue life of a welded structure. *Materials Science and Engineering A*, 595:64–76, 2014. ISSN 09215093. doi: 10.1016/j.msea.2013.11.082. URL `http://dx.doi.org/10.1016/j.msea.2013.11.082`.

X. Cahís, E. Simon, D. Piedrafita, and A. Catalan. Core behavior and low-cycle fatigue estimation of the Perforated Core Buckling-Restrained Brace. *Engineering Structures*, 174(June):126–138, 2018. ISSN 18737323. doi: 10.1016/j.engstruct.2018.07.044.

J. A. F. O. Correia, P. Raposo, M. Muniz-calvente, S. Blasón, G. Lesiuk, A. M. P. D. Jesus, P. M. G. P. Moreira, R. A. B. Calçada, and A. F. Canteli. A generalization of the fatigue Kohout-VeËchet model for several fatigue damage parameters. *Engineering Fracture Mechanics*, 185: 284–300, 2017. ISSN 0013-7944. doi: 10.1016/j.engfracmech.2017.06.009. URL `https://doi.org/10.1016/j.engfracmech.2017.06.009`.

W. Cui. A state of the art review on fatigue life prediction methods for metal structures. *Marine Science annd Technology*, 2002.

R. J. Devaney, P. E. O. Donoghue, and S. B. Leen. Experimental characterisation and computational modelling for cyclic elastic-plastic constitutive behaviour and fatigue damage of X100Q for steel catenary risers. *International Journal of Fatigue*, 116(February):366–378, 2018. ISSN 0142-1123. doi: 10.1016/j.ijfatigue.2018.06.032. URL `https://doi.org/10.1016/j.ijfatigue.2018.06.032`.

C. Garrett and W. Munk. Internal waves in the ocean. *Annu. Rev. Fluid Mech.*, 11(1):339–369, 1979.

G. M. Gemilang, P. A. Reed, and A. J. Sobey. Low-cycle fatigue assessment of offshore mooring chains under service loading. *Marine Structures*, 76(August 2020):102892, 2021. ISSN 09518339. doi: 10.1016/j.marstruc.2020.102892. URL `https://doi.org/10.1016/j.marstruc.2020.102892`.

B. Hamidi Ghaleh Jigh, H. Hosseini-Toudeshky, and M. A. Farsi. Low cycle fatigue analyses of open-celled aluminum foam under compressionâcompression loading using experimental and microstructure finite element analysis. *Journal of Alloys and Compounds*, 797:231–236, 2019. ISSN 09258388. doi: 10.1016/j.jallcom.2019.05.158. URL `https://doi.org/10.1016/j.jallcom.2019.05.158`.

C. Han, X. Qu, Y. Ma, and D. Shi. Experimental and Numerical Study of Fatigue Damage Assessment under Combined High and Low Cycle Loading. *Shock and Vibration*, 2018, 2018. ISSN 10709622. doi: 10.1155/2018/9045658.

R. Hejazi and M. Kimiaei. Equivalent linear soil stiffness in fatigue design of steel catenary risers. *Ocean Engineering*, 111:493–507, 2016. ISSN 0029-8018. doi: 10.1016/j.oceaneng.2015.11.027. URL `http://dx.doi.org/10.1016/j.oceaneng.2015.11.027`.

K. Hou, M. Ou, M. Wang, X. Hao, Y. Ma, and K. Liu. Low cycle fatigue and high cycle fatigue of K4750 Ni-based superalloy at 600 Â°C: Analysis of fracture behavior and deformation mechanism, 2021. ISSN 09215093.

S. V. J. Kohout. A new function for fatigue curves characterization and its multiple merits. 1123 (00), 2001.

C. Jackson and J. Apel. *An atlas of internal solitary-like waves and their properties*. 2004.

L. J. Jia and H. Ge. *Ultra-low-cycle fatigue failure of metal structures under strong earthquakes. Chapter 2 Stress-strain behaviors in large plastic strain ranges under monotonic loading*. 2019. ISBN 978-981-13-2660-8. URL `http://link.springer.com/10.1007/978-981-13-2661-5`.

W. Jiang and P. Yang. Experimental studies on crack propagation and accumulative mean strain of cracked stiffened plates under low-cycle fatigue loads. *Ocean Engineering*, 214(February):107744, 2020. ISSN 00298018. doi: 10.1016/j.oceaneng.2020.107744. URL `https://doi.org/10.1016/j.oceaneng.2020.107744`.

Z. Jiang, Z. Han, and M. Li. A probabilistic model for low-cycle fatigue crack initiation under variable load cycles. *International Journal of Fatigue*, 155(September 2021):106528, 2022. ISSN 01421123. doi: 10.1016/j.ijfatigue.2021.106528. URL `https://doi.org/10.1016/j.ijfatigue.2021.106528`.

J. M. Jonkman and D. Matha. Dynamics of offshore floating wind turbines â analysis of three concepts. *Wind Energy*, (January):557–569, 2011. doi: 10.1002/we.442.

J. C. Kaimal, Y. Izumi, and O. Coté. Spectral characteristics of surface-layer turbulence. pages 563–589, 1972.

C. G. Langner. Offshore Technology Conference 2003. In *Fatigue Life Improvement of Steel Catenary Risers due to Self-Trenching at the Touchdown Point*, Houston, 2003.

J. H. Lee, P. Dong, and M. H. Kim. Low-cycle fatigue evaluation for girth-welded pipes based on the structural strain method considering cyclic material behavior. *International Journal of Naval Architecture and Ocean Engineering*, 12:868–880, 2020. ISSN 20926790. doi: 10.1016/j.ijnaoe.2020.08.005. URL `https://doi.org/10.1016/j.ijnaoe.2020.08.005`.

Z. Li, J. Li, Z. Chen, J. Guo, Y. Zhu, and Y. Luo. Experimental and computational study on thermo-mechanical fatigue life of aluminium alloy piston. *Fatigue and Fracture of Engineering Materials and Structures*, 44(1):141–155, 2021. ISSN 14602695. doi: 10.1111/ffe.13342.

B. Ligaj and G. Szala. Comparative analysis of fatigue life calculation methods of C45 steel in conditions of variable amplitude loads in the low-and high-cycle fatigue ranges. *Polish Maritime Research*, 19(4):23–30, 2012. ISSN 12332585. doi: 10.2478/v10012-012-0037-z.

E. Molinas. *Marés internas e dinâmica sedimentar na plataforma continental amazônica.* PhD thesis, Federal University of Rio de Janeiro., 2020.

E. Molinas, J. Carneiro, , and S. Vinzon. Internal tides as a major process in Amazon continental shelf fine sediment transport. *Marine Geology*, 430(106360), 2020.

W. Neville and P. Sachs. *Practical Plant Failure Analysis*. 2020. ISBN 9781138324114.

A. Orlando, L. Pagnini, and M. P. Repetto. Structural response and fatigue assessment of a small vertical axis wind turbine under stationary and non-stationary excitation. *Renewable Energy*, 170:251–266, 2021. ISSN 0960-1481. doi: 10.1016/j.renene.2021.01.123. URL `https://doi.org/10.1016/j.renene.2021.01.123`.

L. Pomar, M. Morsilli, P. Hallock, and B. Bádenas. Internal waves, an under-explored source of turbulence events in the sedimentary record. *Earth Sci.*, 111(1):56–81, 2012.

L. M. Qu. *EStimating the Fatigue Damage of Steel Catenary Risers*. PhD thesis, 2015.

M. Randolph and P. Quiggin. Non-linear Hysteretic Seabed Model For Catenary Pipeline Contact. In *International Conference on Ocean, Offshore and Artic Engineering 2009, Honolulu, USA, OMAE2009-79259*, 2009.

L. Shaohu, Z. Hao, X. Hui, and G. Quanquan. A new theoretical model of low cycle fatigue life for coiled tubing under coupling load. *Engineering Failure Analysis*, 124(February):105365, 2021. ISSN 13506307. doi: 10.1016/j.engfailanal.2021.105365. URL `https://doi.org/10.1016/j.engfailanal.2021.105365`.

S. M. H. Sharifi, H. Saeidi Googarchin, and F. Forouzesh. Three dimensional analysis of low cycle fatigue failure in engine part subjected to multi-axial variable amplitude thermo-mechanical load. *Engineering Failure Analysis*, 62:128–141, 2016. ISSN 13506307. doi: 10.1016/j.engfailanal.2016.01.003.

A. Sharma, M. C. Oh, and B. Ahn. Recent Advances in Very High Cycle Fatigue Behaviour of Metals and Alloys- A Review, 2020.

H. Shiri. In fl uence of seabed trench formation on fatigue performance of steel catenary risers in touchdown zone. *Marine Structures*, 36:1–20, 2014. ISSN 0951-8339. doi: 10.1016/j.marstruc.2013.12.003. URL `http://dx.doi.org/10.1016/j.marstruc.2013.12.003`.

R. Shoghi and H. Shiri. Modeling touchdown point oscillation and its relationship with fatigue response of steel catenary risers. *Applied Ocean Research*, 87(March):142–154, 2019. ISSN 0141-1187. doi: 10.1016/j.apor.2019.03.010. URL https://doi.org/10.1016/j.apor.2019.03.010.

W. Song, X. Liu, J. Xu, Y. Fan, D. Shi, F. Yang, X. Xia, F. Berto, and D. Wan. Low-Cycle Fatigue Life Prediction of 10CrNi3MoV Steel and Undermatched Welds by Damage Mechanics Approach. *Frontiers in Materials*, 8(April):1–15, 2021. ISSN 22968016. doi: 10.3389/fmats.2021.641145.

M. A. Wahab, I. Hilmy, and R. Hojjati-Talemi. On the use of low and high cycle fatigue damage models. *Key Engineering Materials*, 569-570:1029–1035, 2013. ISSN 16629795. doi: 10.4028/www.scientific.net/KEM.569-570.1029.

J. Wang, S. Fu, R. Baarholm, J. Wu, and C. Martin. Fatigue damage of a steel catenary riser from vortex-induced vibration caused by vessel motions. *Marine Structures*, 39:131–156, 2014. ISSN 0951-8339. doi: 10.1016/j.marstruc.2014.07.002. URL http://dx.doi.org/10.1016/j.marstruc.2014.07.002.

K. Wang, H. Xue, and W. Tang. Time domain prediction approach for cross-flow VIV induced fatigue damage of steel catenary riser near touchdown point. *Elsevier*, 43:166–174, 2013. ISSN 0141-1187. doi: 10.1016/j.apor.2013.09.003. URL http://dx.doi.org/10.1016/j.apor.2013.09.003.

K. Wang, W. Tang, and H. Xue. Time domain approach for coupled cross- fl ow and in-line VIV induced fatigue damage of steel catenary riser at touchdown zone. *Marine Structures*, 41(800):267–287, 2015. ISSN 0951-8339. doi: 10.1016/j.marstruc.2015.02.004. URL http://dx.doi.org/10.1016/j.marstruc.2015.02.004.

J. Xu, S. Benson, and B. Wetenhall. Comparative analysis of fatigue life of a wind turbine yaw bearing with different support foundations. *Ocean Engineering*, 235(October 2020):109293, 2021. ISSN 0029-8018. doi: 10.1016/j.oceaneng.2021.109293. URL https://doi.org/10.1016/j.oceaneng.2021.109293.

B. Yu, A. Gan, and F. J. Masters. Hurricane Wind Power Spectra , Cospectra , and Integral Length Scales. pages 411–430, 2008. doi: 10.1007/s10546-008-9316-8.

Y. Yuan, M. Zheng, H. Xue, and W. Tang. Nonlinear riser-seabed interaction response among touchdown zone of a steel catenary riser in consideration of vortex-induced vibration. *Ocean Engineering*, 227(August 2020):108891, 2021. ISSN 0029-8018. doi: 10.1016/j.oceaneng.2021.108891. URL https://doi.org/10.1016/j.oceaneng.2021.108891.

W. Zhang, L. Zeng, P. Gardoni, and X. Qi. Experimental investigation and low-cycle fatigue behavior of I-shaped steel bracing members with gusset plate connections. *Thin-Walled Structures*, 162(February):107593, 2021. ISSN 02638231. doi: 10.1016/j.tws.2021.107593. URL https://doi.org/10.1016/j.tws.2021.107593.